

Linear Magnetohydrodynamic Waves in a Magneto-Lattice: A Unified Theoretical Framework and Numerical Validation

Shiyu Sun,¹ Peifeng Fan,^{2,*} Yulei Wang,³ Qiang Chen,⁴ Xingkai Li,² and Weihua Wang^{1,†}

¹*Institute of Material Science and Information Technology,*

Anhui University, Hefei, Anhui 230601, China

²*School of Physics, Anhui University, Hefei, Anhui 230601, China*

³*School of Astronomy and Space Science,*

Nanjing University, Nanjing, JiangSu 210023, China

⁴*National Supercomputing Center in Zhengzhou,*

Zhengzhou University, Zhengzhou, Henan 450001, China

Abstract

We present a systematic theoretical and numerical investigation of the propagation properties of linear magnetohydrodynamic (MHD) waves in a spatially periodic magnetic field, referred to as a magneto-lattice. Two types of central equations, expressed in terms of $(\rho, \mathbf{B}, \mathbf{v})$ (where ρ is perturbed mass density, \mathbf{B} is perturbed magnetic field, and \mathbf{v} is perturbed velocity) and the perturbation displacement $\boldsymbol{\xi}$, are established using the plane wave expansion (PWE) method. The validity of both equations is demonstrated through two numerical examples. This framework enables the identification of intrinsic frequency bandgaps and cutoff phenomena within the system. Our numerical results show that the bandgap width increases with the magnetic modulation ratio B_m , leading to the suppression of specific MHD wave modes. Furthermore, the periodicity of the magnetic field induces the splitting of Alfvén waves into multiple branches—a phenomenon absent in uniform plasmas. These findings provide new insights for manipulating MHD waves in a crystalline lattice framework of structured plasmas.

* corresponding author: pffan@ahu.edu.cn

† corresponding author: whwang@ahu.edu.cn

I. INTRODUCTION

The control of wave propagation using spatially periodic structures is a central research direction in modern physics and materials science [1–3]. In particular, periodic mesoscale structures—such as photonic crystals and phononic crystal and have been highly successful in enabling precise manipulation of electromagnetic waves [4–7] and elastic waves [8, 9]. For example, photonic crystals reveal the band splitting and bandgap effects of electromagnetic waves through the periodic spatial arrangement of dielectric constants, providing a theoretical basis for new optical devices [10–17]. Phononic crystals have extended this idea to the field of elastic waves, utilizing the periodic combination of scatterers and substrates to achieve suppression and mode selection of acoustic/elastic wave propagation [18–21]. They have shown great potential in fields such as vibration reduction [22–25], noise reduction [26–30], and acoustic imaging [31–35]. These studies collectively reveal a universal law: spatial periodicity reshapes wave dispersion relations, and the emergence of band gaps enables novel strategies for active wave modulation.

Magnetohydrodynamics (MHD) investigates the macroscopic behavior of electrically conducting fluids in magnetic fields and is widely applied in space physics [36], controlled nuclear fusion [37–39], and astrophysics [40–44]. As the fundamental disturbance modes in magnetized plasmas, MHD waves primarily include fast waves (FWs), slow waves (SWs), and Alfvén waves (AWs). Advances in the understanding of periodic structures have revealed that wave propagation can be profoundly modified by spatial periodicity. In particular, studies of photonic and phononic crystals have shown that periodic structures can give rise to characteristic band gaps (i.e., frequency gaps), within which wave propagation is forbidden. Motivated by this concept, this study explores the propagation behavior of MHD waves in spatially periodic magnetic field structures, referred to as magneto-lattices. This magneto-lattice configuration can be realized either by periodically arranging permanent magnets or by periodically arranging externally energized coils. For instance, Fig. 1(d) illustrates a 2D magneto-lattice formed by a spatially periodic arrangement of magnetic dipoles, analogous to an atomic crystal lattice and conceptually resembling a magnetic crystal.

In this study, we establish a systematic theoretical framework for studying the propagation of linear MHD waves in magneto-lattice. Starting from the ideal MHD equations, we employ a perturbative approach to derive the equilibrium configuration and the correspond-

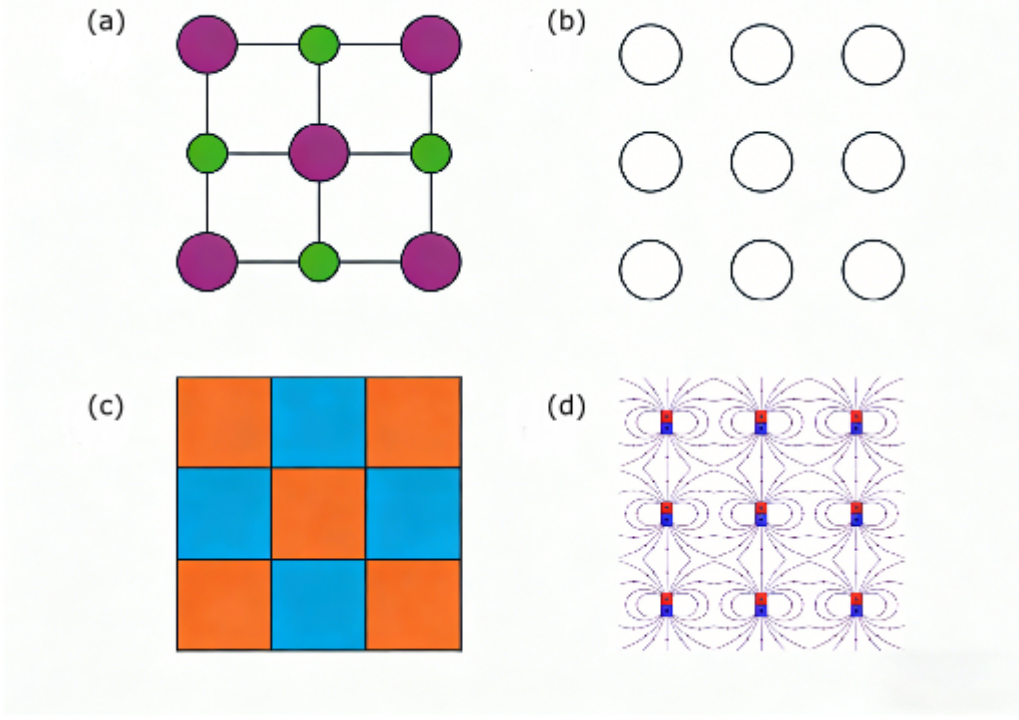


Figure 1. Schematic illustration of periodic lattice structures in different physical systems. (a) Atomic crystal lattice in condensed matter physics. (b) Periodic elastic lattice in a phononic crystal for manipulating acoustic or elastic waves. (c) Periodic dielectric lattice in a photonic crystal for controlling electromagnetic wave propagation. (d) Magneto-lattice formed by periodically arranged magnetic dipoles, producing a spatially modulated magnetic field for controlling the propagation of MHD waves.

ing linearized MHD equations. The magneto-lattice induced equilibrium provides a stable background for MHD wave evolution, analogous to the controlled environments realized in laboratory photonic and phononic crystals. Starting from the linearized MHD equations and applying Bloch's theorem together with the plane wave expansion (PWE) method [45, 46], we systematically derive the central equations in two equivalent representations: one expressed in terms of the perturbed physical fields $(\rho, \mathbf{B}, \mathbf{v})$ (perturbed mass density, magnetic field, and velocity), and the other formulated in terms of the perturbed displacement field $\boldsymbol{\xi}$. To validate the two models, we consider a magnetic field that is uniform in direction (along the y -axis) and sinusoidally modulated in magnitude along the x -direction. The normalized magnetic field is given by $\mathbf{B}_0(x) = [1 + B_m \sin(x)] \mathbf{e}_y$. Two values of the modulation ampli-

tude are considered: $B_m = 0$ corresponding to the empty-lattice (uniform-field) case, and $B_m = 0.1$. The results show excellent agreement between the two theoretical formulations. In addition, full MHD simulations are performed using the Athena++ code [47, 48], with spectral properties extracted via fast Fourier transform (FFT). The simulation results closely match the band-gap locations and widths predicted by the central equations, confirming the effectiveness of periodic magnetic fields in generating band-gaps. Moreover, the numerical results show that periodic magnetic fields can produce substantial frequency gaps, with the band-gap width increasing as the modulation amplitude B_m grows. Notably, Alfvén waves split into multiple branches in a periodic magnetic field—a phenomenon absent in uniform plasma.

The remainder of this paper is organized as follows. Section II reviews the derivation of the MHD equilibrium and ideal linear MHD equations. In Sec. III, we employ the plane wave expansion (PWE) method to derive two central equations for linearized MHD in magneto-lattices. The validation of these formulations, achieved by truncating the central equations and computing dispersion relations for two representative cases, is presented in Sec. IV. Section V compares these results with full MHD simulations conducted using the Athena++ code. Finally, we summarize the main findings and provide a discussion in the concluding section.

II. MHD EQUILIBRIUM AND LINEARIZED EQUATIONS

In electronic materials, crystals are formed by the periodic arrangement of atoms or molecules, which in most cases remains stable and provides a foundational environment for electron motion. Analogously, in MHD systems, the evolution of waves also requires a stable configuration, termed MHD equilibrium. Perturbations propagating atop this equilibrium constitute MHD waves. By extending the concept of a crystal lattice to MHD systems, we aim to establish a spatially periodic equilibrium configuration within a magneto-lattice. Just as electron behavior is described by matter waves or wavefunctions in crystalline structures, MHD waves serve as their counterparts in magnetofluids. Thus, studying MHD waves fundamentally relies on first constructing such equilibrium states, mirroring how investigating "electron waves" necessitates a preexisting crystalline lattice framework.

We begin with the conservative ideal MHD equations [38, 49]

$$\frac{\partial \rho}{\partial t} = -\nabla \cdot (\rho \mathbf{v}), \quad (1)$$

$$\frac{\partial \mathbf{B}}{\partial t} = -\nabla \cdot (\mathbf{v} \mathbf{B} - \mathbf{B} \mathbf{v}), \quad (2)$$

$$\frac{\partial}{\partial t} (\rho \mathbf{v}) = -\nabla \cdot \left[\rho \mathbf{v} \mathbf{v} + \left(P + \frac{\mathbf{B}^2}{8\pi} \right) \mathbf{I} - \frac{\mathbf{B} \mathbf{B}}{4\pi} \right], \quad (3)$$

$$\frac{d}{dt} \left(\frac{P}{\rho^\gamma} \right) = 0, \quad (4)$$

where \mathbf{B} is the magnetic field, γ is the adiabatic index, and ρ , P and \mathbf{v} represent the mass density, thermal pressure, and velocity of the magnetofluid, respectively. Let each physical field be generically denoted as Q , where Q represents quantities such as ρ , P , \mathbf{v} , and others. For a magnetofluid with perturbed fluctuations, each field Q can be decomposed into a stationary equilibrium component Q_0 and a perturbed component Q_1 , i.e., $Q = Q_0 + Q_1$. Since the equilibrium state is time-independent and lacks background flow, (i.e., $\partial Q_0 / \partial t = 0$ and $\mathbf{v}_0 = 0$), the MHD equilibrium equation reduces to

$$\nabla \cdot \left[\left(P_0 + \frac{\mathbf{B}_0^2}{8\pi} \right) \mathbf{I} - \frac{\mathbf{B}_0 \mathbf{B}_0}{4\pi} \right] = 0, \quad (5)$$

which is equivalent to

$$\nabla P_0 = \frac{1}{4\pi} (\nabla \times \mathbf{B}_0) \times \mathbf{B}_0. \quad (6)$$

Substituting $Q = Q_0 + Q_1$ into Eqs. (1)-(4), neglecting higher-order terms, and simplifying the resulting expressions yields the linearized MHD equations governing the perturbations

$$\frac{\partial \rho_1}{\partial t} = -\nabla \cdot (\rho_0 \mathbf{v}_1), \quad (7)$$

$$\frac{\partial \mathbf{B}_1}{\partial t} = -\nabla \cdot (\mathbf{v}_1 \mathbf{B}_0 - \mathbf{B}_0 \mathbf{v}_1), \quad (8)$$

$$\rho_0 \frac{\partial \mathbf{v}_1}{\partial t} = -\nabla \cdot \left[\left(C_s^2 \rho_1 + \frac{\mathbf{B}_0 \cdot \mathbf{B}_1}{4\pi} \right) \mathbf{I} - \frac{\mathbf{B}_0 \mathbf{B}_1 + \mathbf{B}_1 \mathbf{B}_0}{4\pi} \right], \quad (9)$$

where $C_s^2 = \gamma P_0 / \rho_0$ is the sound speed squared.

The linearized MHD equations formulated in terms of the perturbed variables $(\rho_1, \mathbf{B}_1, \mathbf{v}_1)$ involve seven dynamical variables and constitute a system of seven coupled first-order partial differential equations. Alternatively, by introducing the perturbation displacement field $\boldsymbol{\xi}(t, \mathbf{x})$, which satisfies $\mathbf{v}_1 = \partial \boldsymbol{\xi} / \partial t$, the system can be reformulated as three coupled second-order partial differential equations for the components of $\boldsymbol{\xi}$. In this formulation, the lin-

earized MHD equations reduce to a unified governing equation,

$$\rho_0 \frac{\partial^2 \boldsymbol{\xi}}{\partial t^2} = \nabla \cdot \left\{ \left[(\gamma P_0 \nabla \cdot \boldsymbol{\xi} + \boldsymbol{\xi} \cdot \nabla P_0) - \frac{\mathbf{B}_0}{4\pi} \cdot [\nabla \times (\boldsymbol{\xi} \times \mathbf{B}_0)] \right] \mathbf{I} + \frac{\mathbf{B}_0 [\nabla \times (\boldsymbol{\xi} \times \mathbf{B}_0)] + [\nabla \times (\boldsymbol{\xi} \times \mathbf{B}_0)] \mathbf{B}_0}{4\pi} \right\}, \quad (10)$$

where the perturbed fields ρ_1 , P_1 and \mathbf{B}_1 are expressed in terms of $\boldsymbol{\xi}$ as

$$\rho_1 = -\nabla \cdot (\rho_0 \boldsymbol{\xi}), \quad (11)$$

$$P_1 = -\gamma P_0 \nabla \cdot \boldsymbol{\xi} - \boldsymbol{\xi} \cdot \nabla P_0, \quad (12)$$

$$\mathbf{B}_1 = \nabla \times (\boldsymbol{\xi} \times \mathbf{B}_0). \quad (13)$$

Such a displacement-based formulation is widely employed in investigations of MHD instabilities. This displacement-based formulation provides an alternative yet fully equivalent description of linear magnetohydrodynamics and is mathematically equivalent to the original seven-variable first-order system. Accordingly, either Eq. (7)-(9) or equation (10) may be employed to determine the linear perturbations of MHD waves.

Suppose the equilibrium magnetic field \mathbf{B}_0 consists of a uniform background field \mathbf{B}_{0b} and a spatially periodic magneto-lattice component \mathbf{B}_{0L} , so that

$$\mathbf{B}_0(\mathbf{x}) = B_{0b} \mathbf{e}_y + \mathbf{B}_{0L}(\mathbf{x}), \quad (14)$$

The magneto-lattice field \mathbf{B}_{0L} satisfies the periodicity condition $\mathbf{B}_{0L}(\mathbf{x} + \mathbf{R}_n) = \mathbf{B}_{0L}(\mathbf{x})$, where \mathbf{R}_n denotes the lattice vectors. In the absence of \mathbf{B}_{0L} , the equilibrium density and pressure are uniform constants, ρ_{0b} and P_{0b} , respectively. After introducing the magneto-lattice field, the system relaxes to a new equilibrium characterized by spatially periodic mass density ρ_{0L} and pressure P_{0L} which satisfy the equilibrium condition in (5). This establishes a periodic equilibrium. We further assume that the relaxation is isothermal,

$$\frac{P_{0b}}{\rho_{0b}} = \frac{P_0(\mathbf{x})}{\rho_0(\mathbf{x})}, \quad (15)$$

so that the sound speed remains uniform throughout the system, i.e., $C_s^2 = \gamma P_{0b}/\rho_{0b} \equiv C_{sb}^2$, where C_{sb} is the constant background sound speed.

III. CENTRAL EQUATIONS

In condensed matter physics, the central equation plays a fundamental role in the analysis of wave phenomena in periodic media [50]. By exploiting the discrete translational symmetry

of a crystal lattice and combining Bloch's theorem with a PWE, the governing equations can be recast into an eigenvalue problem that explicitly couples different reciprocal lattice vectors. This formulation provides a unified and systematic framework for determining band structures, identifying band gaps, and understanding mode hybridization induced by periodicity. Owing to its generality and transparency, the central equation has become a cornerstone in the theoretical treatment of electrons, phonons, and photonic excitations in crystalline solids.

Motivated by its success in condensed matter systems, we extend this formalism to magnetohydrodynamics in periodic magnetic equilibria. In this section, we derive the central equations for linearized MHD waves in a magneto-lattice, thereby establishing a direct analogy between wave propagation in periodic magnetofluids and that in conventional crystalline materials.

Before deriving the central equations, we nondimensionalize the linearized magnetohydrodynamic equations to obtain a unified, dimensionless formulation. All physical quantities are normalized by the uniform background density ρ_{0b} and magnetic field B_{0b} , and the nondimensional variables are defined as

$$\tilde{\rho}_1 = \frac{\rho_1}{\rho_{0b}}, \tilde{\rho}_{0L} = \frac{\rho_{0L}}{\rho_{0b}}, \tilde{\rho}_0 = \frac{\rho_0}{\rho_{0b}} \quad (16)$$

$$\tilde{\mathbf{B}}_1 = \frac{\mathbf{B}_1}{|B_{0b}|}, \tilde{\mathbf{B}}_{0L} = \frac{\mathbf{B}_{0L}}{|B_{0b}|}, \tilde{\mathbf{B}}_0 = \frac{\mathbf{B}_0}{|B_{0b}|} = \sigma \mathbf{e}_z + \tilde{\mathbf{B}}_{0L}, \quad (17)$$

$$\tilde{\mathbf{v}}_1 = \frac{\mathbf{v}_1}{V_{Ab}}, \quad (18)$$

where $V_{Ab} = \sqrt{B_{0b}^2/4\pi\rho_{0b}}$ is the Alfvén speed and $\sigma = B_{0b}/|B_{0b}| = \pm 1$. Let $s_L = \sqrt[D]{V_{\text{cell}}}/2\pi$ denote the characteristic length of a unit cell, where D is the dimension of the lattice and V_{cell} is the volume of the unit cell. Using s_L and V_{Ab} , the characteristic time is given by $t_0 = s_L/V_{Ab}$, which is referred to as the Alfvén time. The space and time coordinates are nondimensionalized as

$$\tilde{\mathbf{x}} = \frac{\mathbf{x}}{s_L}, \quad \tilde{t} = \frac{t}{t_0}, \quad (19)$$

with the corresponding nondimensional derivatives given by

$$\tilde{\nabla} = s_L \nabla, \quad \frac{\partial}{\partial \tilde{t}} = t_0 \frac{\partial}{\partial t}. \quad (20)$$

Substituting the nondimensional variables from Eqs. (16) and (20) into Eqs. (7) and (9) and omitting tildes “ \sim ” and perturbation subscripts “1” for simplicity, yields the nondimensionalized equations

$$\frac{\partial \rho}{\partial t} = -\nabla \cdot (\rho_0 \mathbf{v}), \quad (21)$$

$$\frac{\partial \mathbf{B}}{\partial t} = -\nabla \cdot (\mathbf{v} \mathbf{B}_0 - \mathbf{B}_0 \mathbf{v}), \quad (22)$$

$$\rho_0 \frac{\partial \mathbf{v}}{\partial t} = -\nabla \cdot [(\beta \rho + \mathbf{B}_0 \cdot \mathbf{B}) \mathbf{I} - (\mathbf{B}_0 \mathbf{B}_1 + \mathbf{B} \mathbf{B}_0)], \quad (23)$$

where $\beta = C_s^2/V_{Ab}^2$ and \mathbf{I} is the identity tensor. The equilibrium condition become

$$\nabla P_0 = \frac{\gamma}{\beta} (\nabla \times \mathbf{B}_0) \times \mathbf{B}_0. \quad (24)$$

Introducing the nondimensional displacement $\tilde{\boldsymbol{\xi}} = \boldsymbol{\xi}/s_L$ and applying the normalization schemes from Eqs. (19) and (20) into Eq. (10), while omitting tildes for brevity, results in

$$\begin{aligned} \rho_0 \frac{\partial^2 \boldsymbol{\xi}}{\partial t^2} = & \nabla \cdot \left\{ \left[\beta \left(\rho_0 \nabla \cdot \boldsymbol{\xi} + \frac{1}{\gamma} \boldsymbol{\xi} \cdot \nabla \rho_0 \right) - \mathbf{B}_0 \cdot \nabla \times (\boldsymbol{\xi} \times \mathbf{B}_0) \right] \mathbf{I} \right. \\ & \left. + \mathbf{B}_0 \nabla \times (\boldsymbol{\xi} \times \mathbf{B}_0) + \nabla \times (\boldsymbol{\xi} \times \mathbf{B}_0) \mathbf{B}_0 \right\}. \end{aligned} \quad (25)$$

A. Central equation in terms of $(\rho, \mathbf{B}, \mathbf{v})$

We next using the PWE method to derive the central equation in terms of $(\rho, \mathbf{B}, \mathbf{v})$. Let $\boldsymbol{\psi}(t, \mathbf{x}) = (\rho, \mathbf{B}, \mathbf{v})$. Assuming time-harmonic solutions, we write $\boldsymbol{\psi}(t, \mathbf{x}) = \boldsymbol{\psi}(\mathbf{x}) e^{-i\omega t}$, where ω is the dimensionless frequency (normalized by t_0 , i.e., $\omega \rightarrow \omega t_0$). Substituting this ansatz into (21)-(23) yields the corresponding eigenvalue equations

$$-i\omega \rho = -\nabla \cdot (\rho_0 \mathbf{v}), \quad (26)$$

$$-i\omega \mathbf{B} = -\nabla \cdot (\mathbf{v} \mathbf{B}_0 - \mathbf{B}_0 \mathbf{v}), \quad (27)$$

$$-i\omega \rho_0 \mathbf{v} = -\nabla \cdot [(\beta \rho + \mathbf{B}_0 \cdot \mathbf{B}) \mathbf{I} - (\mathbf{B}_0 \mathbf{B}_1 + \mathbf{B}_1 \mathbf{B}_0)]. \quad (28)$$

The equilibrium fields (ρ_0, \mathbf{B}_0) , which are spatially periodic with respect to the normalized lattice vectors \mathbf{R}_n (made dimensionless via $\mathbf{R}_n \rightarrow \mathbf{R}_n/s_L$), can be expanded in a Fourier series as

$$(\rho_0, \mathbf{B}_0) = \sum_{\mathbf{G}} (\rho_0 \mathbf{G}, \mathbf{B}_0 \mathbf{G}) e^{i\mathbf{G} \cdot \mathbf{x}}, \quad (29)$$

where \mathbf{G} denotes reciprocal lattice vectors. The corresponding Fourier coefficients are given by

$$(\rho_{0G}, \mathbf{B}_{0G}) = \frac{1}{V_{\text{cell}}} \int_{V_{\text{cell}}} (\rho_0, \mathbf{B}_0) e^{-i\mathbf{G}\cdot\mathbf{x}} d\mathbf{x}. \quad (30)$$

Here, V_{cell} denotes the dimensionless unit-cell volume normalized by s_L^3 , and thus satisfies $V_{\text{cell}} = (2\pi)^3$. Assuming the perturbed fields ψ satisfy periodic boundary conditions throughout the magnetofluid, they can be expanded in a Fourier series of the form:

$$\psi(\mathbf{x}) = \sum_{\mathbf{k}} \psi_{\mathbf{k}} e^{i\mathbf{k}\cdot\mathbf{x}}, \quad (31)$$

where the expansion coefficients $\psi_{\mathbf{k}}$ are given by

$$\psi_{\mathbf{k}} = \frac{1}{V_{\text{cry}}} \int_{V_{\text{cry}}} \psi(\mathbf{x}) e^{-i\mathbf{k}\cdot\mathbf{x}} d\mathbf{x}. \quad (32)$$

Here, V_{cry} represents the dimensionless volume of the whole magnetofluid (normalized by $(s_L/2\pi)^3$), and \mathbf{k} is the discrete wave vector quantized by the periodic boundary conditions.

Substituting Eqs.(29)-Eq.(32) into Eqs.(26)-(28), the continuity equation Eq. (26) becomes

$$\sum_{\mathbf{k}} \omega \rho_{\mathbf{k}} e^{i\mathbf{k}\cdot\mathbf{x}} = \sum_{\mathbf{k}} \sum_{\mathbf{G}} \rho_{0G} (\mathbf{k} + \mathbf{G}) \cdot \mathbf{v}_{\mathbf{k}} e^{i(\mathbf{k} + \mathbf{G})\cdot\mathbf{x}} = \sum_{\mathbf{k}} \sum_{\mathbf{G}} \rho_{0G} \mathbf{k} \cdot \mathbf{v}_{\mathbf{k}-\mathbf{G}} e^{i\mathbf{k}\cdot\mathbf{x}}, \quad (33)$$

where we have redefined the summation index $\mathbf{k} \rightarrow \mathbf{k} - \mathbf{G}$ for each \mathbf{G} in the last step. This is permitted because the sum runs over all wave vectors in the Brillouin zone. Similarly, equation (27) transforms into

$$\begin{aligned} \sum_{\mathbf{k}} \omega \mathbf{B}_{\mathbf{k}} e^{i\mathbf{k}\cdot\mathbf{x}} &= \sum_{\mathbf{k}} \sum_{\mathbf{G}} (\mathbf{k} + \mathbf{G}) \cdot (\mathbf{v}_{\mathbf{k}} \mathbf{B}_{0G} - \mathbf{B}_{0G} \mathbf{v}_{\mathbf{k}}) e^{i(\mathbf{k} + \mathbf{G})\cdot\mathbf{x}} \\ &= \sum_{\mathbf{k}} \sum_{\mathbf{G}} \mathbf{k} \cdot (\mathbf{v}_{\mathbf{k}-\mathbf{G}} \mathbf{B}_{0G} - \mathbf{B}_{0G} \mathbf{v}_{\mathbf{k}-\mathbf{G}}) e^{i\mathbf{k}\cdot\mathbf{x}}. \end{aligned} \quad (34)$$

By manipulating the left-hand side (LHS) of the momentum equation (28) into

$$\sum_{\mathbf{k}} \sum_{\mathbf{G}} \omega \rho_{0G} \mathbf{v}_{\mathbf{k}} e^{i(\mathbf{k} + \mathbf{G})\cdot\mathbf{x}} = \sum_{\mathbf{k}} \sum_{\mathbf{G}} \omega \rho_{0G} \mathbf{v}_{\mathbf{k}-\mathbf{G}} e^{i\mathbf{k}\cdot\mathbf{x}}, \quad (35)$$

equation (28) is then transformed into

$$\sum_{\mathbf{k}} \sum_{\mathbf{G}} \omega \rho_{0G} \mathbf{v}_{\mathbf{k}-\mathbf{G}} e^{i\mathbf{k}\cdot\mathbf{x}} = \sum_{\mathbf{k}} \sum_{\mathbf{G}} [\beta \mathbf{k} \rho_{\mathbf{k}} \delta_{0G} + (\mathbf{k} + \mathbf{G}) (\mathbf{B}_{0G} \cdot \mathbf{B}_{\mathbf{k}})]$$

$$\begin{aligned}
& -(\mathbf{k} + \mathbf{G}) \cdot (\mathbf{B}_{0G}\mathbf{B}_k + \mathbf{B}_k\mathbf{B}_{0G}) \big] e^{i(\mathbf{k} + \mathbf{G}) \cdot \mathbf{x}} \\
& = \sum_{\mathbf{k}} \sum_{\mathbf{G}} [\beta \rho_{\mathbf{k}-\mathbf{G}} \delta_{0G} \mathbf{k} + \mathbf{k} (\mathbf{B}_{0G} \cdot \mathbf{B}_{\mathbf{k}-\mathbf{G}}) \\
& \quad - \mathbf{k} \cdot (\mathbf{B}_{0G}\mathbf{B}_{\mathbf{k}-\mathbf{G}} + \mathbf{B}_{\mathbf{k}-\mathbf{G}}\mathbf{B}_{0G})] e^{i\mathbf{k} \cdot \mathbf{x}}, \tag{36}
\end{aligned}$$

where

$$\delta_{0G} = \begin{cases} 1 & \mathbf{G} = 0, \\ 0 & \mathbf{G} \neq 0. \end{cases} \tag{37}$$

By invoking the uniqueness of Fourier decompositions in Eqs. (33), (34) and (36), we derive the central equations

$$\sum_{\mathbf{G}} (-\omega \delta_{0G} \rho_{\mathbf{k}-\mathbf{G}} + \rho_{0G} \mathbf{k} \cdot \mathbf{v}_{\mathbf{k}-\mathbf{G}}) = 0, \tag{38}$$

$$\sum_{\mathbf{G}} [-\omega \delta_{0G} \mathbf{B}_{\mathbf{k}-\mathbf{G}} + \mathbf{k} \cdot (\mathbf{v}_{\mathbf{k}-\mathbf{G}} \mathbf{B}_{0G} - \mathbf{B}_{0G} \mathbf{v}_{\mathbf{k}-\mathbf{G}})] = 0, \tag{39}$$

$$\sum_{\mathbf{G}} [-\omega \rho_{0G} \mathbf{v}_{\mathbf{k}-\mathbf{G}} + \beta \delta_{0G} \mathbf{k} \rho_{\mathbf{k}-\mathbf{G}} + \mathbf{k} (\mathbf{B}_{0G} \cdot \mathbf{B}_{\mathbf{k}-\mathbf{G}}) - \mathbf{k} \cdot (\mathbf{B}_{0G}\mathbf{B}_{\mathbf{k}-\mathbf{G}} + \mathbf{B}_{\mathbf{k}-\mathbf{G}}\mathbf{B}_{0G})] = 0. \tag{40}$$

These equations can be compactly expressed in matrix form

$$\sum_{\mathbf{G}} \mathcal{N}(\omega, \mathbf{k}, \mathbf{G}) \cdot \psi_{\mathbf{k}-\mathbf{G}} = 0, \tag{41}$$

where the tensor $\mathcal{N}(\omega, \mathbf{k}, \mathbf{G})$ is defined as

$$\mathcal{N}(\omega, \mathbf{k}, \mathbf{G}) \equiv \begin{pmatrix} -\omega \delta_{0G} & 0 & \rho_{0G} \mathbf{k} \\ 0 & -\omega \delta_{0G} \mathbf{I} & \mathbf{B}_{0G} \mathbf{k} - (\mathbf{k} \cdot \mathbf{B}_{0G}) \mathbf{I} \\ \beta \delta_{0G} \mathbf{k} & (\mathbf{k} \mathbf{B}_{0G} - \mathbf{B}_{0G} \mathbf{k}) - (\mathbf{k} \cdot \mathbf{B}_{0G}) \mathbf{I} & -\omega \rho_{0G} \mathbf{I} \end{pmatrix}, \tag{42}$$

which constitutes a 7×7 matrix in any given Cartesian coordinate system and can be rewritten as

$$\mathcal{N}(\omega, \mathbf{k}, \mathbf{G}) = \begin{pmatrix} -\omega \delta_{0G} & 0 & 0 & 0 & \rho_{0G} k_x & \rho_{0G} k_y & \rho_{0G} k_z \\ 0 & -\omega \delta_{0G} & 0 & 0 & -B_{0G} k_y & 0 & 0 \\ 0 & 0 & -\omega \delta_{0G} & 0 & B_{0G} k_x & 0 & B_{0G} k_z \\ 0 & 0 & 0 & -\omega \delta_{0G} & 0 & 0 & -B_{0G} k_y \\ \beta \delta_{0G} k_x & -B_{0G} k_y & B_{0G} k_x & 0 & -\omega \rho_{0G} & 0 & 0 \\ \beta \delta_{0G} k_y & -B_{0G} k_x & -B_{0G} k_y & -B_{0G} k_z & 0 & -\omega \rho_{0G} & 0 \\ \beta \delta_{0G} k_z & 0 & B_{0G} k_z & -B_{0G} k_y & 0 & 0 & -\omega \rho_{0G} \end{pmatrix}. \tag{43}$$

Consider the "empty-lattice" case where the lattice field modulation amplitude $\mathbf{B}_{0L} = 0$. In this scenario, the entire magnetofluid is uniform: the equilibrium magnetic field $\mathbf{B}_0 = \mathbf{B}_{0b}$ and mass density ρ_0 are spatially constant. For normalization, we set $\mathbf{B}_{0b} = \mathbf{e}_y$ and $\rho_0 = 1$. Notably, only the reciprocal lattice vector $\mathbf{G} = 0$ contributes non-zero Fourier coefficients: specifically, $(\rho_{0G}, \mathbf{B}_{0G}) = (1, \mathbf{e}_y)$ when $\mathbf{G} = 0$, while $(\rho_{0G}, \mathbf{B}_{0G}) = (0, \mathbf{0})$ for all $\mathbf{G} = 0$. Under these uniform-field conditions, Eq. (41) reduces to

$$\begin{pmatrix} \ddots & 0 & 0 & 0 & 0 \\ 0 & \mathcal{N}(\omega, \mathbf{k} + \mathbf{G}_0, 0) & 0 & 0 & 0 \\ 0 & 0 & \mathcal{N}(\omega, \mathbf{k}, 0) & 0 & 0 \\ 0 & 0 & 0 & \mathcal{N}(\omega, \mathbf{k} - \mathbf{G}_0, 0) & 0 \\ 0 & 0 & 0 & 0 & \ddots \end{pmatrix} \begin{pmatrix} \vdots \\ \psi_{\mathbf{k} + \mathbf{G}_0} \\ \psi_{\mathbf{k}} \\ \psi_{\mathbf{k} - \mathbf{G}_0} \\ \vdots \end{pmatrix} = 0, \quad \mathbf{k} \in 1_{st}BZ, \quad (44)$$

where \mathbf{G}_0 denotes each reciprocal lattice vector in reciprocal space. The nontrivial solutions of Eq. (44) imply

$$\cdots (\det \mathcal{N}(\omega, \mathbf{k} + \mathbf{G}_0, 0)) \cdot (\det \mathcal{N}(\omega, \mathbf{k}, 0)) \cdot (\det \mathcal{N}(\omega, \mathbf{k} - \mathbf{G}_0, 0)) \cdots = 0, \quad (45)$$

where $\mathbf{k} \in 1_{st}BZ$, equivalently, this condition can be reduced to

$$\cdots = \det \mathcal{N}(\omega, \mathbf{k} + \mathbf{G}_0, 0) = \det \mathcal{N}(\omega, \mathbf{k}, 0) = \det \mathcal{N}(\omega, \mathbf{k} - \mathbf{G}_0, 0) = \cdots = 0, \quad (46)$$

Accordingly, equation (46) can be equivalently rewritten in the compact form

$$\det \mathcal{N}(\omega, \mathbf{k}, 0) = 0, \quad \mathbf{k} \in BZ. \quad (47)$$

The difference between Eqs. (45) and (47) lies in the domain of \mathbf{k} : in the former \mathbf{k} is restricted to the first Brillouin zone, whereas in the latter, \mathbf{k} spans the full Brillouin zone. Assuming the By calculating this determinant we obtain the dispersion equation as

$$\omega (\omega^2 - k_y^2) [\omega^4 - (1 + \beta^2) k^2 \omega^2 + \beta^2 k_y^2 k^2] = 0, \quad (48)$$

where $k^2 = k_z^2 + k_y^2 + k_z^2$. The result of Eqs. (48) is consistent with the well known results [51].

Equation (48) can be readily solved as

$$\omega = 0, \quad (49)$$

$$\omega = \pm k_y, \quad (50)$$

$$\omega^2 = \frac{k^2}{2} \left[(1 + \beta) + \sqrt{(1 + \beta)^2 - 4\beta k_y^2/k^2} \right], \quad (51)$$

$$\omega^2 = \frac{k^2}{2} \left[(1 + \beta) - \sqrt{(1 + \beta)^2 - 4\beta k_y^2/k^2} \right]. \quad (52)$$

Here, equations (50)-(52) describe the AWs, FWs and SWs, respectively. Equation (49) corresponds to the zero-frequency mode, which are often not examined in standard theoretical analyses.

B. Central equation in terms of ξ

Given the utility of formulating MHD equations in terms of ξ , and to benchmark this formulation against the previously derived central equations for $(\rho, \mathbf{B}, \mathbf{v})$, we now derive the central equation in terms of ξ . This derivation builds upon the theoretical framework established in Subsec. III A, thereby ensuring the equivalence and complementarity of the two central equation expressions. We begin with Eq. (25). Building on the methodology employed in the preceding subsection, we assume a time-harmonic form for the perturbed displacement field, i.e., $\xi(t, \mathbf{x}) = \xi(\mathbf{x}) e^{-i\omega t}$. Substituting this ansatz into Eq. (25), yields the eigenvalue equation

$$-\omega^2 \rho \xi = \nabla \cdot \left\{ \left[\beta \left(\rho_0 \nabla \cdot \xi + \frac{1}{\gamma} \xi \cdot \nabla \rho_0 \right) - \mathbf{B}_0 \cdot \nabla \times (\xi \times \mathbf{B}_0) \right] \mathbf{I} + \mathbf{B}_0 \nabla \times (\xi \times \mathbf{B}_0) + \nabla \times (\xi \times \mathbf{B}_0) \mathbf{B}_0 \right\}. \quad (53)$$

Assuming the perturbed displacement field ξ satisfies periodic boundary conditions over the magnetofluid domain, it can be expanded in a Fourier series as

$$\xi(\mathbf{x}) = \sum_{\mathbf{k}} \xi_{\mathbf{k}} e^{i\mathbf{k} \cdot \mathbf{x}}, \quad (54)$$

where the wave vector \mathbf{k} is quantized by the periodicity, and the expansion coefficients are given by the inverse transform

$$\xi_{\mathbf{k}} = \frac{1}{V_{\text{cry}}} \int_{V_{\text{cry}}} \xi(\mathbf{x}) e^{-i\mathbf{k} \cdot \mathbf{x}} d\mathbf{x}. \quad (55)$$

By substituting Eqs. (29) and (54) into Eq. (53), and following a procedure analogous to that in Subsec. III A, we obtain the central equation for ξ . This requires expanding each term in Eq. (53) using the PWE method

$$-\omega^2 \rho_0 \boldsymbol{\xi} = -\omega^2 \sum_{\mathbf{k}} \sum_{\mathbf{G}} \rho_{0\mathbf{G}} \boldsymbol{\xi}_{\mathbf{k}-\mathbf{G}} e^{i\mathbf{k}\cdot\mathbf{x}}, \quad (56)$$

$$\nabla \times (\boldsymbol{\xi} \times \mathbf{B}_0) = \sum_{\mathbf{k}} \sum_{\mathbf{G}} i \mathbf{k} \times (\boldsymbol{\xi}_{\mathbf{k}-\mathbf{G}} \times \mathbf{B}_{0\mathbf{G}}) e^{i\mathbf{k}\cdot\mathbf{x}}, \quad (57)$$

$$\begin{aligned} \mathbf{B}_0 \nabla \times (\boldsymbol{\xi} \times \mathbf{B}_0) &= \sum_{\mathbf{k}} \sum_{\mathbf{G}} \sum_{\mathbf{G}'} i \mathbf{B}_{0\mathbf{G}'} \left\{ \left[(\mathbf{k} - \mathbf{G}') \cdot \mathbf{B}_{0\mathbf{G}} \right] \boldsymbol{\xi}_{\mathbf{k}-\mathbf{G}-\mathbf{G}'} \right. \\ &\quad \left. - \mathbf{B}_{0\mathbf{G}} (\mathbf{k} - \mathbf{G}') \cdot \boldsymbol{\xi}_{\mathbf{k}-\mathbf{G}-\mathbf{G}'} \right\} e^{i\mathbf{k}\cdot\mathbf{x}}, \end{aligned} \quad (58)$$

$$\begin{aligned} \mathbf{B}_0 \cdot \nabla \times (\boldsymbol{\xi} \times \mathbf{B}_0) &= \sum_{\mathbf{k}} \sum_{\mathbf{G}} \sum_{\mathbf{G}'} i \left\{ \left[(\mathbf{k} - \mathbf{G}') \cdot \mathbf{B}_{0\mathbf{G}} \right] \mathbf{B}_{0\mathbf{G}'} \right. \\ &\quad \left. - (\mathbf{B}_{0\mathbf{G}} \cdot \mathbf{B}_{0\mathbf{G}'}) (\mathbf{k} - \mathbf{G}') \right\} \cdot \boldsymbol{\xi}_{\mathbf{k}-\mathbf{G}-\mathbf{G}'} e^{i\mathbf{k}\cdot\mathbf{x}}, \end{aligned} \quad (59)$$

$$\begin{aligned} \nabla \times (\boldsymbol{\xi} \times \mathbf{B}_0) \mathbf{B}_0 &= \sum_{\mathbf{k}} \sum_{\mathbf{G}} \sum_{\mathbf{G}'} i \left\{ \left[(\mathbf{k} - \mathbf{G}') \cdot \mathbf{B}_{0\mathbf{G}} \right] \boldsymbol{\xi}_{\mathbf{k}-\mathbf{G}-\mathbf{G}'} \right. \\ &\quad \left. - \mathbf{B}_{0\mathbf{G}} (\mathbf{k} - \mathbf{G}') \cdot \boldsymbol{\xi}_{\mathbf{k}-\mathbf{G}-\mathbf{G}'} \right\} \mathbf{B}_{0\mathbf{G}'} e^{i\mathbf{k}\cdot\mathbf{x}}, \end{aligned} \quad (60)$$

$$\beta \left(\rho_0 \nabla \cdot \boldsymbol{\xi} + \frac{1}{\gamma} \boldsymbol{\xi} \cdot \nabla \rho_0 \right) = \sum_{\mathbf{k}} \sum_{\mathbf{G}} \sum_{\mathbf{G}'} i \beta \delta_{0\mathbf{G}'} \rho_{0\mathbf{G}} \left(\mathbf{k} - \frac{\gamma-1}{\gamma} \mathbf{G} \right) \cdot \boldsymbol{\xi}_{\mathbf{k}-\mathbf{G}-\mathbf{G}'} e^{i\mathbf{k}\cdot\mathbf{x}}. \quad (61)$$

Substituting Eq. (56)-Eq. (61) into Eq. (53) yields the following eigenvalue equation

$$\begin{aligned} &-\omega^2 \sum_{\mathbf{k}} \sum_{\mathbf{G}} \rho_{0\mathbf{G}} \boldsymbol{\xi}_{\mathbf{k}-\mathbf{G}} e^{i\mathbf{k}\cdot\mathbf{x}} \\ &= - \sum_{\mathbf{k}} \sum_{\mathbf{G}} \sum_{\mathbf{G}'} \left\{ \beta \rho_{0\mathbf{G}} \delta_{0\mathbf{G}'} \mathbf{k} \left(\mathbf{k} - \frac{\gamma-1}{\gamma} \mathbf{G} \right) \right. \\ &\quad - \left[(\mathbf{k} - \mathbf{G}') \cdot \mathbf{B}_{0\mathbf{G}} \right] \mathbf{k} \mathbf{B}_{0\mathbf{G}'} + (\mathbf{B}_{0\mathbf{G}} \cdot \mathbf{B}_{0\mathbf{G}'}) \mathbf{k} (\mathbf{k} - \mathbf{G}') \\ &\quad + \left[(\mathbf{k} \cdot \mathbf{B}_{0\mathbf{G}'}) (\mathbf{k} - \mathbf{G}') \cdot \mathbf{B}_{0\mathbf{G}} \right] \mathbf{I} - (\mathbf{k} \cdot \mathbf{B}_{0\mathbf{G}'}) \mathbf{B}_{0\mathbf{G}} (\mathbf{k} - \mathbf{G}') \\ &\quad \left. + \left[(\mathbf{k} - \mathbf{G}') \cdot \mathbf{B}_{0\mathbf{G}} \right] \mathbf{B}_{0\mathbf{G}'} \mathbf{k} - (\mathbf{k} \cdot \mathbf{B}_{0\mathbf{G}}) \mathbf{B}_{0\mathbf{G}'} (\mathbf{k} - \mathbf{G}') \right\} \cdot \boldsymbol{\xi}_{\mathbf{k}-\mathbf{G}-\mathbf{G}'} e^{i\mathbf{k}\cdot\mathbf{x}}. \end{aligned} \quad (62)$$

By invoking the uniqueness of Fourier decompositions in Eq. (62), we derive the central equations

$$\sum_{\mathbf{G}} \sum_{\mathbf{G}'} \mathcal{M}(\omega, \mathbf{k}, \mathbf{G}, \mathbf{G}') \cdot \boldsymbol{\xi}_{\mathbf{k}-\mathbf{G}-\mathbf{G}'} = 0, \quad (63)$$

where $\mathcal{M}(\omega, \mathbf{k}, \mathbf{G}, \mathbf{G}')$ is defined as

$$\mathcal{M}(\omega, \mathbf{k}, \mathbf{G}, \mathbf{G}') = \mathcal{H}(\mathbf{k}, \mathbf{G}, \mathbf{G}') - \omega^2 \rho_{0\mathbf{G}} \delta_{0\mathbf{G}'} \mathbf{I}, \quad (64)$$

and where $\mathcal{H}(\mathbf{k}, \mathbf{G}, \mathbf{G}')$ is given by

$$\begin{aligned}\mathcal{H}(\mathbf{k}, \mathbf{G}, \mathbf{G}') &= \beta \rho_{0\mathbf{G}} \delta_{0\mathbf{G}'} \mathbf{k} \left(\mathbf{k} - \frac{\gamma-1}{\gamma} \mathbf{G} \right) - \left[(\mathbf{k} - \mathbf{G}') \cdot \mathbf{B}_{0\mathbf{G}} \right] \mathbf{k} \mathbf{B}_{0\mathbf{G}'} \\ &+ (\mathbf{B}_{0\mathbf{G}} \cdot \mathbf{B}_{0\mathbf{G}'}) \mathbf{k} (\mathbf{k} - \mathbf{G}') + \left[(\mathbf{k} \cdot \mathbf{B}_{0\mathbf{G}'}) (\mathbf{k} - \mathbf{G}') \cdot \mathbf{B}_{0\mathbf{G}} \right] \mathbf{I} \\ &- (\mathbf{k} \cdot \mathbf{B}_{0\mathbf{G}'}) \mathbf{B}_{0\mathbf{G}} (\mathbf{k} - \mathbf{G}') + \left[(\mathbf{k} - \mathbf{G}') \cdot \mathbf{B}_{0\mathbf{G}} \right] \mathbf{B}_{0\mathbf{G}'} \mathbf{k} - (\mathbf{k} \cdot \mathbf{B}_{0\mathbf{G}}) \mathbf{B}_{0\mathbf{G}'} (\mathbf{k} - \mathbf{G}').\end{aligned}\quad (65)$$

Similar to Subsec. (III A), we consider “empty lattice” case. Under this condition, Eqs (63) becomes

$$\begin{pmatrix} \ddots & 0 & 0 & 0 & 0 \\ 0 & \mathcal{M}(\omega, \mathbf{k} + \mathbf{G}_0, 0, 0) & 0 & 0 & 0 \\ 0 & 0 & \mathcal{M}(\omega, \mathbf{k}, 0, 0) & 0 & 0 \\ 0 & 0 & 0 & \mathcal{M}(\omega, \mathbf{k} - \mathbf{G}_0, 0, 0) & 0 \\ 0 & 0 & 0 & 0 & \ddots \end{pmatrix} \begin{pmatrix} \vdots \\ \xi_{\mathbf{k} + \mathbf{G}_0} \\ \xi_{\mathbf{k}} \\ \xi_{\mathbf{k} - \mathbf{G}_0} \\ \vdots \end{pmatrix} = 0, \quad \mathbf{k} \in 1_{st} BZ, \quad (66)$$

For nontrivial solutions, this further leads to

$$\cdots (\det \mathcal{M}(\omega, \mathbf{k} + \mathbf{G}_0, 0, 0)) \cdot (\det \mathcal{M}(\omega, \mathbf{k}, 0, 0)) \cdot (\det \mathcal{M}(\omega, \mathbf{k} - \mathbf{G}_0, 0, 0)) \cdots = 0, \quad \mathbf{k} \in 1_{st} BZ. \quad (67)$$

Equation (67) can be equivalently rewritten as

$$\det \mathcal{M}(\omega, \mathbf{k}, 0, 0) = 0, \quad \mathbf{k} \in BZ. \quad (68)$$

Evaluating this determinant yields

$$(\omega^2 - k_y^2) [\omega^4 - (1 + \beta) k^2 \omega^2 + \beta k_y^2 k^2] = 0. \quad (69)$$

The result of Eq. (69) is consistent with that of Eq. (48), with the only exception being the absence of the $\omega = 0$ solution.

IV. TRUNCATED CENTRAL EQUATIONS AND BAND STRUCTURE IN A SINUSSOIDAL MAGNETO-LATTICE

With the central equations formally established, we proceed to their numerical implementation for calculating the wave band structure in a magneto-lattice. For a simple yet

non-trivial configuration, we construct a magneto-lattice by superimposing a spatially sinusoidal magnetic field onto a uniform background, the normalized equilibrium magnetic field in this setup is then given by

$$\mathbf{B}_0(x) = [1 + B_m \sin(x)] \mathbf{e}_y. \quad (70)$$

Here, we take $\sigma = 1$. The normalized equilibrium pressure and density are defined respectively as

$$P_0(x) = 1 + P_{0L}(x), \quad (71)$$

$$\rho_0(x) = 1 + \rho_{0L}(x). \quad (72)$$

To satisfy the MHD equilibrium condition (5), $P_0(x)$ and $\rho_0(x)$ must be consistent with $\mathbf{B}_0(x)$. Substituting Eq. (71) into Eq. (24) yields the balance relation

$$\frac{d}{dx} P_0(x) = -\frac{\gamma}{\beta} B_0(x) \frac{dB_0(x)}{dx}. \quad (73)$$

Integrating with respect to x gives the explicit equilibrium pressure

$$P_0(x) = 1 + \frac{\gamma}{\beta} \left[-B_m \sin(x) + \frac{B_m^2}{4} \cos(2x) \right]. \quad (74)$$

Assuming the lattice field relaxes under isothermal conditions Eq. (15), the normalized equilibrium density follows directly as

$$\rho_0(x) = 1 + \frac{\gamma}{\beta} \left[-B_m \sin(x) + \frac{B_m^2}{4} \cos(2x) \right]. \quad (75)$$

Having derived Eqs. (70) and (75), the Fourier components of \mathbf{B}_0 and ρ_0 can be calculated by using Eqs. (30), which is listed in the following table.

Table I. Fourier coefficients of magnetic fields and densities for different G values

G	≤ -2	-2	-1	0	1	2	≥ 2
ρ_{0G}	0	$\frac{\gamma}{8\beta} B_m^2$	$-\frac{\gamma}{2\beta} i B_m$	0	$\frac{\gamma}{2\beta} i B_m$	$\frac{\gamma}{8\beta} B_m^2$	0
$ \mathbf{B}_{0G} $	0	0	$-\frac{1}{2} i B_m$	0	$-\frac{1}{2} i B_m$	0	0

Although the central Eq. (41) and Eq. (63) theoretically describe the propagation behavior of linear MHD waves in a magneto-lattice, they are formally infinite dimensional as

they involve the coupling of all reciprocal lattice vectors \mathbf{G} , making direct numerical solution infeasible. To convert this into a computable finite dimensional matrix eigenvalue problem, truncation of the reciprocal lattice vector set is necessary. We proceed to calculate the dispersion equation and determine the band structure of this 1D magneto-lattice using the central equation formulated in terms of $(\rho, \mathbf{B}, \mathbf{v})$ (see Eq. (41)). Focusing on the region covered by the first Brillouin zone, we specifically limit the reciprocal lattice vectors \mathbf{G} to $0, \pm 1, \pm 2$, thereby truncating the infinite sum in the central equation into a numerically tractable finite form.

$$\sum_{G=-2}^2 \mathcal{N}(\omega, k_x, k_y, k_z, G) \cdot \psi_{k_x-G} = 0, \quad (76)$$

where fixed values are adopted for k_y and k_z . To solve for all possible ψ_{k_x} , we first fold all energy bands into the first Brillouin zone, such that $k_x \in 1_{st}BZ$. This folding, combined with the truncation introduced earlier, transforms the central equation into a system of three coupled equations

$$\begin{aligned} \mathcal{N}(\omega, k_x - 1, 0) \cdot \psi_{k_x-1} + \mathcal{N}(\omega, k_x - 1, -1) \cdot \psi_{k_x} + \mathcal{N}(\omega, k_x - 1, -2) \cdot \psi_{k_x+1} &= 0, \\ \mathcal{N}(\omega, k_x, 1) \cdot \psi_{k_x-1} + \mathcal{N}(\omega, k_x, 0) \cdot \psi_{k_x} + \mathcal{N}(\omega, k_x, -1) \cdot \psi_{k_x+1} &= 0, \\ \mathcal{N}(\omega, k_x + 1, 2) \cdot \psi_{k_x-1} + \mathcal{N}(\omega, k_x + 1, 1) \cdot \psi_{k_x} + \mathcal{N}(\omega, k_x + 1, 0) \cdot \psi_{k_x+1} &= 0. \end{aligned} \quad (77)$$

To determine the dispersion relation, we require the system of equations to have a non-trivial solution, which imposes the condition that the determinant of the coefficient matrix must be zero. This leads to the following dispersion equation

$$\det \begin{pmatrix} \mathcal{N}(\omega, k_x - 1, 0) & \mathcal{N}(\omega, k_x - 1, -1) & \mathcal{N}(\omega, k_x - 1, -2) \\ \mathcal{N}(\omega, k_x, 1) & \mathcal{N}(\omega, k_x, 0) & \mathcal{N}(\omega, k_x, -1) \\ \mathcal{N}(\omega, k_x + 1, 2) & \mathcal{N}(\omega, k_x + 1, 1) & \mathcal{N}(\omega, k_x + 1, 0) \end{pmatrix} = 0. \quad (78)$$

To benchmark the ξ based central equation against the $(\rho, \mathbf{B}, \mathbf{v})$ based formulation developed in the preceding section, we now implement the identical truncation strategy for the ξ dependent system. Consistent with the truncation method employed for the $(\rho, \mathbf{B}, \mathbf{v})$ equations, we limit the reciprocal lattice vectors \mathbf{G} and \mathbf{G}' to $0, \pm 1, \pm 2$. The central equation (63) can thus be truncated as

$$\sum_{G=-2}^2 \sum_{G'=-2}^{-2} \mathcal{M}(\omega, k_x, k_y, k_z, G, G') \cdot \boldsymbol{\xi}_{k_x-G-G'} = 0. \quad (79)$$

Following the identical procedure applied to the $(\rho, \mathbf{B}, \mathbf{v})$ formulation above, we fold the perturbed displacement components $\boldsymbol{\xi}_{k_x}$ into the first Brillouin zone, such that $k_x \in 1_{st}BZ$. Similar to the procedure in deriving Eq. (77), equation (79) can be transformed into three coupled equations

$$\begin{aligned} \Theta(\omega, k_x - 1, 0) \cdot \boldsymbol{\xi}_{k_x-1} + \Theta(\omega, k_x - 1, -1) \cdot \boldsymbol{\xi}_{k_x} + \Theta(\omega, k_x - 1, -2) \cdot \boldsymbol{\xi}_{k_x+1} &= 0, \\ \Theta(\omega, k_x, 1) \cdot \boldsymbol{\xi}_{k_x-1} + \Theta(\omega, k_x, 0) \cdot \boldsymbol{\xi}_{k_x} + \Theta(\omega, k_x, -1) \cdot \boldsymbol{\xi}_{k_x+1} &= 0, \\ \Theta(\omega, k_x + 1, 2) \cdot \boldsymbol{\xi}_{k_x-1} + \Theta(\omega, k_x + 1, 1) \cdot \boldsymbol{\xi}_{k_x} + \Theta(\omega, k_x + 1, 0) \cdot \boldsymbol{\xi}_{k_x+1} &= 0, \end{aligned} \quad (80)$$

where Θ are defined as

$$\begin{aligned} \Theta(\omega, k_x, k_y, k_z, 0) &= \mathcal{M}(\omega, k_x, k_y, k_z, 1, -1) + \mathcal{M}(\omega, k_x, k_y, k_z, -1, 1) + \mathcal{M}(\omega, k_x, k_y, k_z, 0, 0) \\ \Theta(\omega, k_x, k_y, k_z, 1) &= \mathcal{M}(\omega, k_x, k_y, k_z, 0, 1) + \mathcal{M}(\omega, k_x, k_y, k_z, 1, 0) \\ \Theta(\omega, k_x, k_y, k_z, -1) &= \mathcal{M}(\omega, k_x, k_y, k_z, 0, -1) + \mathcal{M}(\omega, k_x, k_y, k_z, -1, 0) \\ \Theta(\omega, k_x, k_y, k_z, 2) &= \mathcal{M}(\omega, k_x, k_y, k_z, 2, 0) + \mathcal{M}(\omega, k_x, k_y, k_z, 0, 2) + \mathcal{M}(\omega, k_x, k_y, k_z, 1, 1) \\ \Theta(\omega, k_x, k_y, k_z, -2) &= \mathcal{M}(\omega, k_x, k_y, k_z, -2, 0) + \mathcal{M}(\omega, k_x, k_y, k_z, 0, -2) + \mathcal{M}(\omega, k_x, k_y, k_z, -1, -1) \end{aligned} \quad (81)$$

The corresponding dispersion equation thus can be obtained by setting the determinant of the coefficient matrix to zero:

$$\det \begin{pmatrix} \Theta(\omega, k_x + 1, 0) & \Theta(\omega, k_x + 1, 1) & \Theta(\omega, k_x + 1, 2) \\ \Theta(\omega, k_x, -1) & \Theta(\omega, k_x, 0) & \Theta(\omega, k_x, 1) \\ \Theta(\omega, k_x - 1, -2) & \Theta(\omega, k_x - 1, -1) & \Theta(\omega, k_x - 1, 0) \end{pmatrix} = 0. \quad (82)$$

The band structure, or equivalently the dispersion relations, can be calculated using Eq. (78) or Eq. (82), respectively. As a benchmark of the two truncated models, we consider two cases, $B_m = 0$ and $B_m = 0.1$, and solve Eqs. (78) and (82) numerically using Python. The results are shown in Fig. 2, demonstrating excellent agreement between the two central equation models. Results from the two formulations are plotted on the same graphs and distinguished by solid dots and hollow circles. As seen in Fig. (2), the solid dots are nearly

coincident with the hollow circles, indicating strong consistency between the two dispersion relations. To further quantify the agreement, we analyze the error distribution between the two central equations. The maximum discrepancy remains on the order of 10^{-3} for different values of B_m . This confirms that the differences between the two formulations are well within an acceptable range.

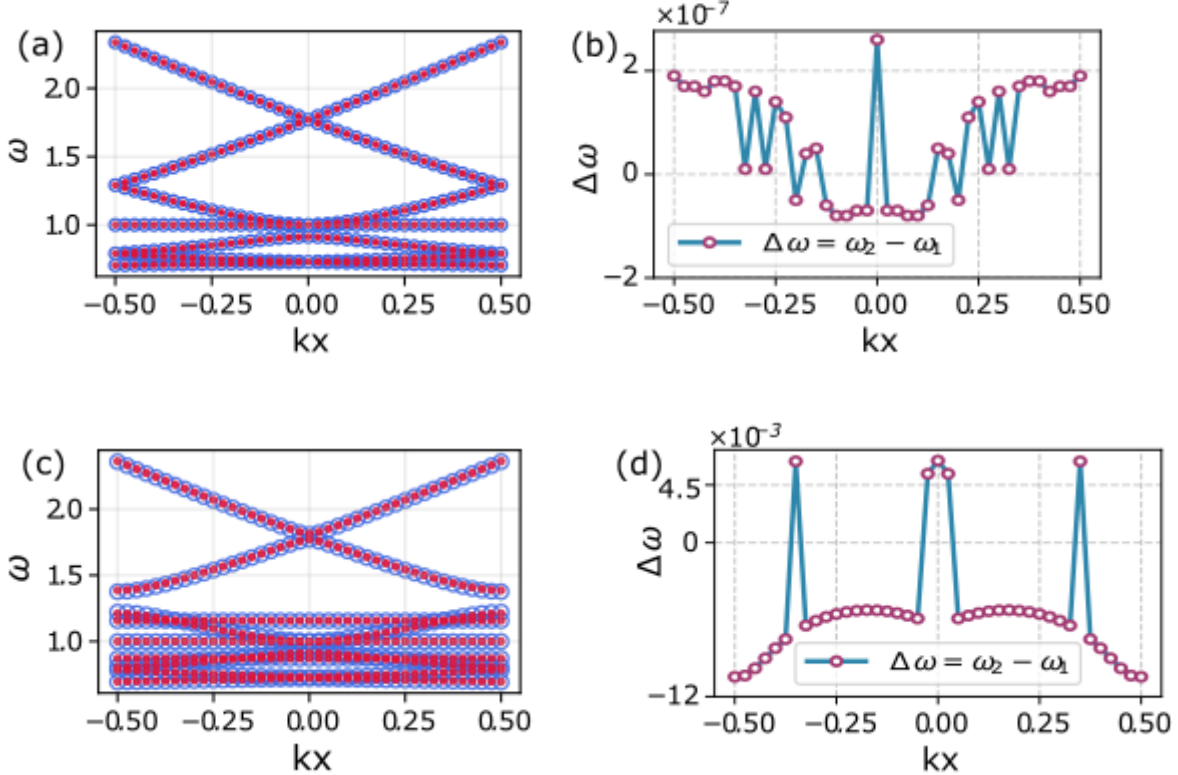


Figure 2. Band-structure (dispersion-relation) benchmark for two central equations with $k_y = 1$ and $k_z = 0$. (a) Dispersion relations at $B_m = 0$. Hollow circles and solid dots denote results obtained from the $(\rho, \mathbf{B}, \mathbf{v})$, formulation and the ξ formulation, respectively. (b) Maximum frequency difference $\Delta\omega$ between the two dispersion relations as a function of k_x at $B_m = 0$. (c) Same as (a), but for $B_m = 0.1$. (d) Same as (b), but for $B_m = 0.1$.

V. FULL MHD SIMULATIONS

The direct numerical simulations were performed using the Athena++ code [47]. The computational domain was set to $x \in [-280\pi, 280\pi]$, $y \in [-\pi, \pi]$, and $z \in [-1, 1]$, discretized

with a mesh of $8192 \times 64 \times 1$ cells. This configuration prioritizes high resolution along the direction of magnetic field modulation x while maintaining computational efficiency. The plasma was modeled with the adiabatic index $\gamma = 5/3$ and the parameter of $\beta = 5/6$. The computational domain is designed with periodic boundary conditions applied globally. To excite a broad spectrum of linear waves, initial velocity perturbations were imposed: for v_x , 500 random disturbance points were seeded in the x -direction and 30 in the y -direction; for v_z , 30 points were seeded in x and 3 in y , all within the amplitude range of $(-0.001, 0.001)$. Each simulation ran for a total of 500 Alfvén time. For spectral analysis, we selected wavenumbers with k_x in $[-1.5, 1.5]$, k_y near 1 and k_z near 0 with the resulting bands folded into the first Brillouin zone for direct analysis.

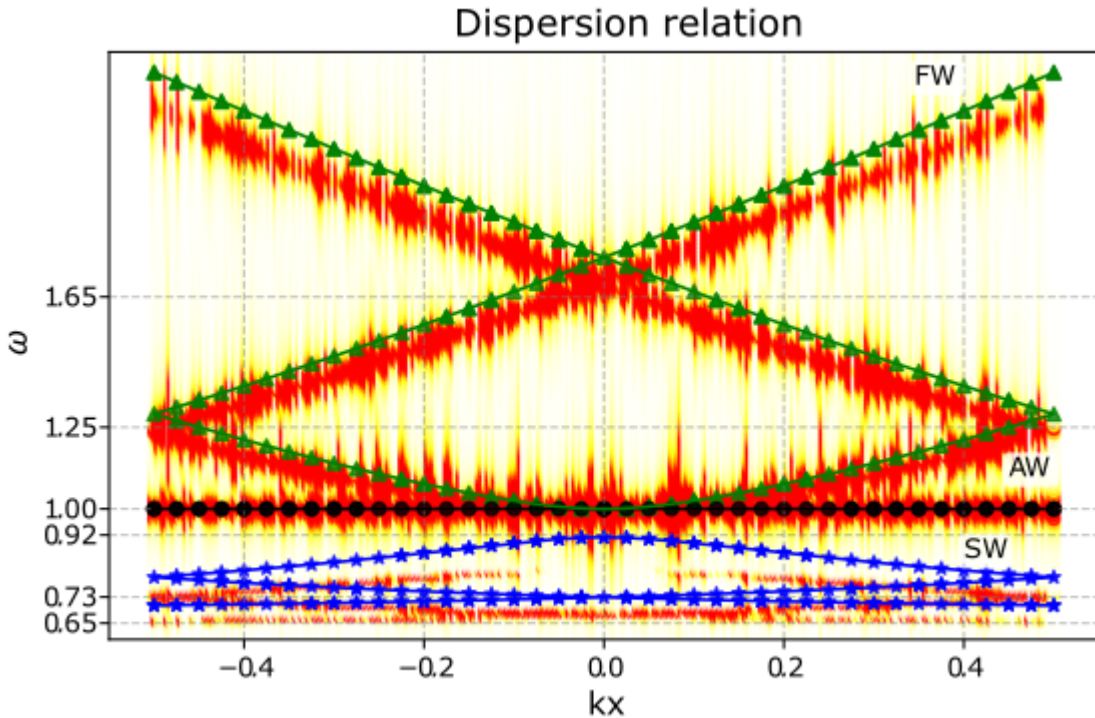


Figure 3. Comparison of results from three models under the empty lattice approximation. The solid curves represent the analytical solution, the discrete points represent the results from the truncated central equations, and the heatmap represents the background power spectrum of the full MHD simulation performed with the Athena++ code. The dispersion relations for fast waves, slow waves, and Alfvén waves were calculated individually and subsequently folded into the first Brillouin zone.

We first computed the band structure via the empty lattice approximation introduced in

Sec. IV, i.e., with $B_m = 0$ and $\mathbf{B}_0 = \mathbf{e}_y$. We employed three distinct models: the full MHD model governed by the ideal MHD equations, the analytical model referenced in Eq. (49)-(52), and the truncated central equation model referenced in Eq. (78) or Eq. (82). Benchmark results are presented in Fig. 3, where the background power spectrum, discrete points, and solid curves correspond to the results of the full MHD model, truncated central equation model, and analytical model, respectively. The findings demonstrate excellent consistency across all three models.

We next computed the band structure using the truncated central equation and full MHD simulations for sinusoidal periodic magnetic modulation with $B_m = 0.1$ and $B_m = 0.2$. The results are summarized in Fig. 4. The discrete points represent the results derived from the truncated central equation (78), while the heatmaps of the power spectrum correspond to the full MHD evolution simulated with the Athena++ code. The power spectrum of the FWs and AWs are extracted through fast Fourier transformation (FFT) of the velocity fields $v_x(t, \mathbf{x})$ and $v_z(t, \mathbf{x})$ respectively, with both velocity fields obtained from the Athena++ simulations. The truncated model shows good agreement with the full MHD simulations regarding the key spectral characteristics of both wave types.

As illustrated in Fig. 4, the distinct physical phenomena induced by periodic magnetic modulation are clearly exhibited. For the case of $B_m = 0.1$, a prominent frequency bandgap appears in the FWs branch [Fig. 4(a)], which corresponds to the suppression of wave propagation within a specific frequency range. This suppression is a direct result of the spatial periodicity of the magneto-lattice. Meanwhile, the AWs branch splits into discrete sub-branches [Fig. 4(b)], an effect that is absent in uniform plasmas. When the modulation amplitude is increased to $B_m = 0.2$, the width of the FWs bandgap increases [Fig. 4(c)], and the splitting of the AWs branch becomes more pronounced [Fig. 4(d)]. These results confirm that the intensity of the effects induced by such periodicity is positively correlated with B_m . The above observations demonstrate that the propagation of MHD waves can be tunably modulated by periodic magnetic structures, where the adjustable bandgaps allow for the targeted suppression of undesirable wave modes.

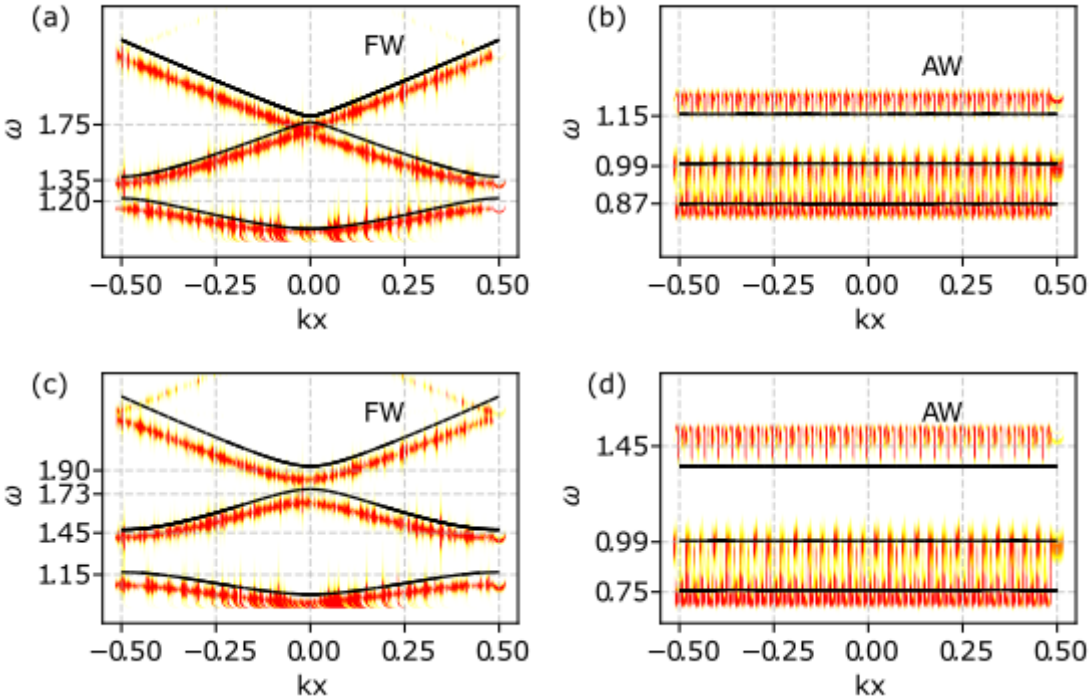


Figure 4. Comparison between Athena++ simulations and the truncated central equation. The solid line represents the result from the truncated central equation, while the power spectrum shows the numerical result from the Athena++ simulation. (a) fast wave with $B_m = 0.1$, (b) Alfvén wave with $B_m = 0.1$, (c) fast wave with $B_m = 0.2$, (d) Alfvén wave with $B_m = 0.2$.

VI. CONCLUSION AND DISCUSSION

This study establishes a systematic theoretical and numerical framework for analyzing linear MHD wave propagation in magneto-lattices. Starting from the ideal MHD equations, we review the perturbative approach to obtain the equilibrium configuration and linearized MHD equations. The MHD equilibrium holds fundamental importance in this research, and its role is equivalent to that of crystalline lattices in condensed matter physics and periodic structures in photonic and phononic crystals. The linearized MHD equations are used in two distinct yet equivalent forms, one is a set of first order partial differential equations expressed in terms of $(\rho, \mathbf{B}, \mathbf{v})$, and the other is a system of second-order partial differential equations formulated on the basis of the perturbation displacement $\boldsymbol{\xi}$. The presence of a periodic magnetic field induces a periodic equilibrium state, and this equilibrium plays a pivotal role in modulating the propagation of plasma waves. By analogy with theoretical

models in condensed matter physics, we generally derive two equivalent central equations based on the $(\rho, \mathbf{B}, \mathbf{v})$ and the perturbation displacement $\boldsymbol{\xi}$, through the PWE method, and these two central equations serve as the fundamental equations for calculating the dispersion relations and band structures of MHD waves.

As a special scenario, we conduct several verification studies under a 1D sinusoidally modulated magnetic field to demonstrate the reliability of the model. First, we conduct comparative verification of the two models represented by $(\rho, \mathbf{B}, \mathbf{v})$ and $\boldsymbol{\xi}$, truncate the central equations using the same truncation method to obtain their truncated versions, adopt the empty lattice approximation, and calculate the band structures with the two truncated central equations, which show good agreement between them as well as with theoretical analytical solutions, a consistency that is also maintained when setting $B_m = 0.1$. We further verify the validity of the truncation scheme by conducting full MHD simulations, where we introduce random values of v_x and v_z at the initial moment, evolve the system for 500 Alfvén times, perform FFT analysis on the obtained physical quantities, and the results are in good agreement with those from the truncated central equations, which further confirms the effectiveness of our model. These two central equations successfully reveal intrinsic frequency bandgaps and cutoff phenomena in the system, with the bandgap width increasing with the magnetic modulation amplitude B_m , and the presence of the magneto-lattice induces the splitting of AWs modes into multiple branches, an effect that is absent in uniform plasmas.

These findings provide new theoretical insights for controlling MHD waves in structured plasmas, and in future work, we will apply this model to study the band structures and propagation characteristics of MHD waves in 2D or 3D magneto-lattices, such as spatially periodic magnetic islands, and analyze the nonlinear behaviors arising when the magnetic field intensity of the magneto-lattice is comparable to that of the background magnetic field.

ACKNOWLEDGMENTS

P. F. is grateful to Dr. Zhaoyang Liu, Dr. Jianyuan Xiao, Dr. Jinhong Yang, and Dr. Zhenzhen Ren for fruitful discussions. This work is supported by the National Natural

Science Foundation of China (Grant No. 12275001 and 12473057).

- [1] F. Zangeneh-Nejad and R. Fleury, *Reviews in Physics* **4**, 100031 (2019).
- [2] Z.-K. Lin, Q. Wang, Y. Liu, H. Xue, B. Zhang, Y. Chong, and J.-H. Jiang, *Nature Reviews Physics* **5**, 483 (2023).
- [3] F. Yang, Z. Zhang, L. Xu, Z. Liu, P. Jin, P. Zhuang, M. Lei, J. Liu, J.-H. Jiang, X. Ouyang, F. Marchesoni, and J. Huang, *Reviews of Modern Physics* **96**, 015002 (2024).
- [4] Z. Zhang and S. Satpathy, *Phys. Rev. Lett.* **65**, 2650 (1990).
- [5] J. D. Joannopoulos, P. R. Villeneuve, and S. Fan, *Nature* **386**, 143 (1997).
- [6] L. Maigyte and K. Staliunas, *Applied Physics Reviews* **2**, 011102 (2015).
- [7] H.-F. Zhang, S.-B. Liu, and X.-K. Kong, *Physics of Plasmas* **19**, 122103 (2012).
- [8] P. Wang, L. Lu, and K. Bertoldi, *Physical Review Letters* **115**, 104302 (2015).
- [9] S.-N. Liang, J.-L. Xie, C. He, S.-Y. Yu, and Y.-F. Chen, *Physical Review B* **111**, 184103 (2025).
- [10] L. C. Botten, T. P. White, C. M. de Sterke, and R. C. McPhedran, *Physical Review E* **74**, 026603 (2006).
- [11] R. V. Nair and R. Vijaya, *Progress in Quantum Electronics* **34**, 89 (2010).
- [12] L. Maigyte and K. Staliunas, *Applied Physics Reviews* **2**, 011102 (2015).
- [13] H. Shen, Z. Wang, Y. Wu, and B. Yang, *RSC Advances* **6**, 4505 (2016).
- [14] V. G. Baryshevsky and A. A. Gurinovich, *Physical Review Accelerators and Beams* **22**, 044702 (2019).
- [15] M. Butt, S. Khonina, and N. Kazanskiy, *Optics & Laser Technology* **142**, 107265 (2021).
- [16] Z.-W. Luo, H. Ji, X. Jin, J. Song, Z.-Q. Yu, P. Duan, and T. Zhao, *Nature Communications* **16**, 9960 (2025).
- [17] Y. Jin, E. Lucas, J. Zang, T. Briles, I. Dickson, D. Carlson, and S. B. Papp, *Nature Communications* **16**, 5077 (2025).
- [18] M. Badreddine Assouar and M. Oudich, *Applied Physics Letters* **99**, 123505 (2011).
- [19] M. I. Hussein and e. Leamy, *Applied Mechanics Reviews* **66**, 040802 (2014).
- [20] B. J. Ash, S. R. Worsfold, P. Vukusic, and G. R. Nash, *Nature Communications* **8**, 174 (2017).

[21] T. Vasileiadis, J. Varghese, V. Babacic, J. Gomis-Bresco, D. Navarro Urrios, and B. Graczykowski, *Journal of Applied Physics* **129**, 160901 (2021).

[22] D. Yu, J. Wen, H. Zhao, Y. Liu, and X. Wen, *Journal of Sound & Vibration* **318**, 193 (2008).

[23] P. Xiao, L. Miao, H. Zheng, B. Zhang, L. Lei, J. Zhang, and T. Geng, *Applied Physics A: Materials Science* **131**, 19 (2010).

[24] O. R. Bilal, D. Ballagi, and C. Daraio, *Physical Review Applied* **10**, 054060 (2018).

[25] P. Xiao, L. Miao, H. Zheng, and L. Lei, *Construction and Building Materials* **411**, 134734 (2024).

[26] N. K. Batra, P. Matic, and R. K. Everett, in *Ultrasonics Symposium* (2002).

[27] J. Wu, F. Ma, S. Zhang, and L. Shen, *Journal of Mechanical Engineering* **52**, 68 (2016).

[28] Y. Pan, R. Liu, G. Bin, and X. He, *Applied Acoustics* **200**, 109075 (2022).

[29] S. M. F. Rizvi, K. Wang, F. E. Jalal, J. Wu, and A. Al-Mansour, *Scientific Reports* **15**, 18054 (2025).

[30] Z. A. Zaky, M. El Malki, I. Antraoui, A. Khettabi, and M. Sallah, *Scientific Reports* **15**, 16597 (2025).

[31] D. M. Profunser, O. B. Wright, and O. Matsuda, *Physical Review Letters* **97**, 055502 (2006).

[32] J. Li, Z. Liu, and C. Qiu, *Phys. Rev. B* **73**, 054302 (2006).

[33] C. Qiu, X. Zhang, and Z. Liu, *Physical Review B* **71**, 054302 (2005).

[34] F. Ma, Z. Huang, C. Liu, and J. H. Wu, *Journal of Applied Physics* **131**, 011103 (2022).

[35] P. Beoletto, F. Nistri, A. Gliozzi, N. Pugno, and F. Bosia, *Physical Review Applied* **22**, 064054 (2024).

[36] Y. Zhou, W. Matthaeus, and P. Dmitruk, *Reviews of Modern Physics* **76**, 1015 (2004).

[37] J. P. Freidberg, *Rev. Mod. Phys.* **54**, 801 (1982).

[38] J. P. Freidberg, *Ideal MHD* (Cambridge University, New York, 2014).

[39] J. Ongena, R. Koch, R. Wolf, and H. Zohm, *Nature Physics* **12**, 398 (2016).

[40] G. Nigro, F. Malara, V. Carbone, and P. Veltri, *Physical Review Letters* **92**, 194501 (2004).

[41] M. Yamada, R. Kulsrud, and H. Ji, *Reviews of Modern Physics* **82**, 603 (2010).

[42] S. Lebedev, A. Frank, and D. Ryutov, *Reviews of Modern Physics* **91**, 025002 (2019).

[43] V. M. Nakariakov and D. Y. Kolotkov, *Annual Review of Astronomy and Astrophysics* **58**, 441 (2020).

- [44] X. Zhou, Y. Shen, D. Yuan, R. Keppens, X. Zhao, L. Fu, Z. Tang, J. Wang, and C. Zhou, *Nature Communications* **15**, 3281 (2024).
- [45] Y.-C. Hsue, A. J. Freeman, and B.-Y. Gu, *Physical Review B* **72**, 195118 (2005).
- [46] V. F. D. Poggetto and A. L. Serpa, *International Journal of Mechanical Sciences* **184**, 105841 (2020).
- [47] J. M. Stone, K. Tomida, C. J. White, and K. G. Felker, *The Astrophysical Journal Supplement Series* **249**, 4 (2020).
- [48] Athena++ development team, “Athena++,” (2021), available at <https://github.com/PrincetonUniversity/athena/releases/tag/v21.0>.
- [49] G. Visconti and P. Ruggieri, “Fluid dynamics,” (Springer International Publishing, Cham, 2020) pp. 287–322.
- [50] C. Kittel, “Introduction to solid state physics,” (John Wiley & Sons, New York, 1979) pp. 169–182.
- [51] M. Hirota and Y. Fukumoto, *Journal of Mathematical Physics* **49**, 083101 (2008).